

*Physics**Physics Research Publications*

*Purdue University**Year 2010*

Measurement of the η $b(1S)$ mass and
the branching fraction for $\Gamma(3S)$
 $\rightarrow \gamma \eta b(1S)$

G. Bonvicini, D. Cinabro, A. Lincoln, M. J. Smith, P. Zhou, J. Zhu, P. Naik, J. Rademacker, D. M. Asner, K. W. Edwards, J. Reed, A. N. Robichaud, G. Tatishvili, E. J. White, R. A. Briere, H. Vogel, P. U. E. Onyisi, J. L. Rosner, J. P. Alexander, D. G. Cassel, R. Ehrlich, L. Fields, R. S. Galik, L. Gibbons, S. W. Gray, D. L. Hartill, B. K. Heltsley, J. M. Hunt, D. L. Kreinick, V. E. Kuznetsov, J. Ledoux, H. Mahlke-Kruger, J. R. Patterson, D. Peterson, D. Riley, A. Ryd, A. J. Sadoff, X. Shi, S. Stroiney, W. M. Sun, J. Yelton, P. Rubin, N. Lowrey, S. Mehrabyan, M. Selen, J. Wiss, M. Kornicer, R. E. Mitchell, M. R. Shepherd, C. M. Tarbert, D. Besson, T. K. Pedlar, J. Xavier, D. Cronin-Hennessy, K. Y. Gao, J. Hietala, R. Poling, P. Zweber, S. Dobbs, Z. Metreveli, K. K. Seth, B. J. Y. Tan, A. Tomaradze, S. Brisbane, J. Libby, L. Martin, A. Powell, P. Spradlin, C. Thomas, G. Wilkinson, H. Mendez, J. Y. Ge, D. H. Miller, I. P. J. Shipsey, B. Xin, G. S. Adams, D. Hu, B. Moziak, J. Napolitano, K. M. Ecklund, J. Insler, H. Muramatsu, C. S. Park, E. H. Thorndike, F. Yang, M. Artuso, S. Blusk, S. Khalil, R. Mountain, K. Randrianarivony, T. Skwarnicki, J. C. Wang, L. M. Zhang, and C. Collaboration

This paper is posted at Purdue e-Pubs.

http://docs.lib.purdue.edu/physics_articles/1178

Measurement of the $\eta_b(1S)$ mass and the branching fraction for $Y(3S) \rightarrow \gamma\eta_b(1S)$

G. Bonvicini,¹ D. Cinabro,¹ A. Lincoln,¹ M. J. Smith,¹ P. Zhou,¹ J. Zhu,¹ P. Naik,² J. Rademacker,² D. M. Asner,³ K. W. Edwards,³ J. Reed,³ A. N. Robichaud,³ G. Tashvili,³ E. J. White,³ R. A. Briere,⁴ H. Vogel,⁴ P. U. E. Onyisi,⁵ J. L. Rosner,⁵ J. P. Alexander,⁶ D. G. Cassel,⁶ R. Ehrlich,⁶ L. Fields,⁶ R. S. Galik,⁶ L. Gibbons,⁶ S. W. Gray,⁶ D. L. Hartill,⁶ B. K. Heltsley,⁶ J. M. Hunt,⁶ D. L. Kreinick,⁶ V. E. Kuznetsov,⁶ J. Ledoux,⁶ H. Mahlke-Krüger,⁶ J. R. Patterson,⁶ D. Peterson,⁶ D. Riley,⁶ A. Ryd,⁶ A. J. Sadoff,⁶ X. Shi,⁶ S. Stroiney,⁶ W. M. Sun,⁶ J. Yelton,⁷ P. Rubin,⁸ N. Lowrey,⁹ S. Mehrabyan,⁹ M. Selen,⁹ J. Wiss,⁹ M. Kornicer,¹⁰ R. E. Mitchell,¹⁰ M. R. Shepherd,¹⁰ C. M. Tarbert,¹⁰ D. Besson,¹¹ T. K. Pedlar,¹² J. Xavier,¹² D. Cronin-Hennessy,¹³ K. Y. Gao,¹³ J. Hietala,¹³ R. Poling,¹³ P. Zweber,¹³ S. Dobbs,¹⁴ Z. Metreveli,¹⁴ K. K. Seth,¹⁴ B. J. Y. Tan,¹⁴ A. Tomaradze,¹⁴ S. Brisbane,¹⁵ J. Libby,¹⁵ L. Martin,¹⁵ A. Powell,¹⁵ P. Spradlin,¹⁵ C. Thomas,¹⁵ G. Wilkinson,¹⁵ H. Mendez,¹⁶ J. Y. Ge,¹⁷ D. H. Miller,¹⁷ I. P. J. Shipsey,¹⁷ B. Xin,¹⁷ G. S. Adams,¹⁸ D. Hu,¹⁸ B. Moziak,¹⁸ J. Napolitano,¹⁸ K. M. Ecklund,¹⁹ J. Insler,²⁰ H. Muramatsu,²⁰ C. S. Park,²⁰ E. H. Thorndike,²⁰ F. Yang,²⁰ M. Artuso,²¹ S. Blusk,²¹ S. Khalil,²¹ R. Mountain,²¹ K. Randrianarivony,²¹ T. Skwarnicki,²¹ J. C. Wang,²¹ and L. M. Zhang²¹

(CLEO Collaboration)

¹Wayne State University, Detroit, Michigan 48202, USA²University of Bristol, Bristol BS8 1TL, UK³Carleton University, Ottawa, Ontario, Canada K1S 5B6⁴Carnegie Mellon University, Pittsburgh, Pennsylvania 15213, USA⁵University of Chicago, Chicago, Illinois 60637, USA⁶Cornell University, Ithaca, New York 14853, USA⁷University of Florida, Gainesville, Florida 32611, USA⁸George Mason University, Fairfax, Virginia 22030, USA⁹University of Illinois, Urbana-Champaign, Illinois 61801, USA¹⁰Indiana University, Bloomington, Indiana 47405, USA¹¹University of Kansas, Lawrence, Kansas 66045, USA¹²Luther College, Decorah, Iowa 52101, USA¹³University of Minnesota, Minneapolis, Minnesota 55455, USA¹⁴Northwestern University, Evanston, Illinois 60208, USA¹⁵University of Oxford, Oxford OX1 3RH, UK¹⁶University of Puerto Rico, Mayaguez, Puerto Rico 00681¹⁷Purdue University, West Lafayette, Indiana 47907, USA¹⁸Rensselaer Polytechnic Institute, Troy, New York 12180, USA¹⁹Rice University, Houston, Texas 77005, USA²⁰University of Rochester, Rochester, New York 14627, USA²¹Syracuse University, Syracuse, New York 13244, USA

(Received 29 September 2009; published 24 February 2010)

We report evidence for the ground state of bottomonium, $\eta_b(1S)$, in the radiative decay $Y(3S) \rightarrow \gamma\eta_b$ in e^+e^- annihilation data taken with the CLEO III detector. Using 6×10^6 $Y(3S)$ decays, and assuming $\Gamma(\eta_b) = 10 \pm 5 \text{ MeV}/c^2$, we obtain $\mathcal{B}(Y(3S) \rightarrow \gamma\eta_b) = (7.1 \pm 1.8 \pm 1.3) \times 10^{-4}$, where the first error is statistical and the second is systematic. The statistical significance is $\sim 4\sigma$. The mass is determined to be $M(\eta_b) = 9391.8 \pm 6.6 \pm 2.0 \text{ MeV}/c^2$, which corresponds to the hyperfine splitting $\Delta M_{\text{hf}}(1S)_b = 68.5 \pm 6.6 \pm 2.0 \text{ MeV}/c^2$. Using 9×10^6 $Y(2S)$ decays, we place an upper limit on the corresponding $Y(2S)$ decay, $\mathcal{B}(Y(2S) \rightarrow \gamma\eta_b) < 8.4 \times 10^{-4}$ at 90% confidence level.

DOI: 10.1103/PhysRevD.81.031104

PACS numbers: 14.40.-n, 12.38.Qk, 13.25.Gv

The spectroscopy of the $b\bar{b}$ bottomonium states provides valuable insight into Quantum Chromodynamics (QCD) since relativistic and higher-order α_s corrections are less important for $b\bar{b}$ than any other $q\bar{q}$ system. Experimental measurements of the spectroscopic properties of the bottomonium states can therefore be compared with greater

confidence with the predictions of perturbative QCD, as well as with lattice calculations. The hyperfine mass splitting of the singlet-triplet states is of particular interest since it probes the spin-dependent properties of the $q\bar{q}$ system.

The triplet S state (1^3S_1) of $b\bar{b}$ bottomonium, $Y(1S)$, was discovered 30 years ago, but the identification of its

partner, the singlet S state (1^1S_0), $\eta_b(1S)$ (henceforth η_b), has eluded numerous searches, including those by CUSB [1], ALEPH [2], DELPHI [3], and CLEO [4]. As a result, the $1S$ hyperfine splitting, which is well-determined in the charmonium system, remained unknown in the bottomonium system. Recently, using their data sample of 109×10^6 $Y(3S)$ events, the *BABAR* collaboration reported [5,6] the observation of the η_b with a statistical significance of more than 10σ (standard deviations) in the inclusive photon spectrum of $Y(3S)$ with the observed photon energy $E_\gamma(Y(3S) \rightarrow \gamma\eta_b) = 921.2_{-2.8}^{+2.1} \pm 2.4$ MeV, where the first error is statistical and the second is systematic. This gave $M(\eta_b) = 9388.9_{-2.3}^{+3.1} \pm 2.7$ MeV/ c^2 and a bottomonium hyperfine splitting, $\Delta M_{\text{hf}}(1S)_b \equiv M(Y(1S)) - M(\eta_b) = 71.4_{-2.3}^{+3.1} \pm 2.7$ MeV/ c^2 . *BABAR*'s measured branching fraction was $\mathcal{B}(Y(3S) \rightarrow \gamma\eta_b) = (4.8 \pm 0.5 \pm 0.6) \times 10^{-4}$. Corroboration of the *BABAR* finding with an independent data set is essential.

In this article we reexamine the CLEO data for the radiative decays $Y(3S, 2S) \rightarrow \gamma\eta_b$. An earlier analysis of the same data resulted in upper limits of $\mathcal{B}(Y(3S) \rightarrow \gamma\eta_b) < 4.3 \times 10^{-4}$ and $\mathcal{B}(Y(2S) \rightarrow \gamma\eta_b) < 5.1 \times 10^{-4}$ at 90% confidence level [4]. However, the analysis had shortcomings which are rectified in this article. The presence of the photon line corresponding to initial state radiation (ISR), $e^+e^- \rightarrow \gamma Y(1S)$, located between the $\chi_{bJ}(2P, 1P) \rightarrow \gamma Y(1S)$ region and the η_b signal region, was not included in the fits to the inclusive photon spectrum, an omission which biased the result toward small branching fractions. The assumption of $\Gamma(\eta_b) = 0$ MeV had a similar effect. Moreover, the analysis did not employ an important background-suppression variable, the angle between the radiative photon and the thrust axis of the rest of the event, introduced by *BABAR* [5]. We improve upon the previous publication by exploiting a more complete understanding of the expected photon line shape over a broad energy range to more accurately represent the $\chi_{bJ}(2P, 1P) \rightarrow \gamma Y(1S)$, ISR, and η_b (with nonzero width) signals in a fit. We also employ a broader range of binning, fit ranges, and background parametrizations in order to avoid bias in any of these choices.

The CLEO III detector, which has been described elsewhere [7], contains a CsI electromagnetic calorimeter, an inner silicon vertex detector, a central drift chamber, and a ring-imaging Cherenkov (RICH) detector, inside a superconducting solenoid magnet with a 1.5 T magnetic field. The detector has a total acceptance of 93% of 4π . The photon energy resolution in the central (83% of 4π) part of the calorimeter is about 2% at $E_\gamma = 1$ GeV and about 5% at 100 MeV. The charged particle momentum resolution is about 0.6% at 1 GeV/ c .

The CLEO data sets correspond to $(5.88 \pm 0.12) \times 10^6$ $Y(3S)$ and $(9.32 \pm 0.19) \times 10^6$ $Y(2S)$ decays. Our event selection for the inclusive photon spectra is identical to that reported in Ref. [4]. Events are required to have one or

more photons, and three or more charged tracks. Photons with $E_\gamma \geq 20$ MeV are accepted in the ‘‘good barrel’’ region of the calorimeter with $|\cos\theta| < 0.81$ (where θ is the polar angle with respect to the incoming positron direction). Each photon is required to have a transverse spread which is consistent with that of an electromagnetic shower. Photons from π^0 decays are suppressed by vetoing any photon candidates that, when paired with another photon candidate in the good barrel or ‘‘good endcap’’ ($0.85 < |\cos\theta| < 0.93$) regions, have a mass within 2.5σ of the known π^0 mass and $\cos\theta_{\gamma\gamma} > 0.7$, where $\theta_{\gamma\gamma}$ is the opening angle of the photon candidates in the lab frame.

We first consider the analysis of the inclusive photon spectrum from $Y(3S)$ decays. The analysis of $Y(2S)$ decays follows a similar path. In the region $500 < E_\gamma < 1200$ MeV, the spectrum consists of a peak centered around $E_\gamma \approx 770$ MeV due to the three unresolved transitions, $\chi_{bJ}(2P) \rightarrow \gamma Y(1S)$, $J = 0, 1, 2$ on top of a smooth background that falls sharply with energy. The peaks due to ISR and η_b , which are more than an order of magnitude weaker than those from $\chi_{bJ}(2P)$, are expected in the high energy tail region of the $\chi_{bJ}(2P)$ peak. Hence, sensitivity to the possible presence of an η_b signal depends critically upon properly representing the shape of the $\chi_{bJ}(2P)$ peaks as well as suppressing the underlying smooth background (as already achieved in part by the π^0 veto). As demonstrated by the *BABAR* analysis [5], additional suppression can be achieved by recognizing that η_b signal photons are largely uncorrelated in direction with the rest of the event, whereas background photons from the continuum tend to follow the leading particles of the underlying event. This effect is more pronounced for $Y(3S) \rightarrow \gamma\eta_b$ decays than for $Y(2S) \rightarrow \gamma\eta_b$, but the effect is nevertheless useful for background suppression in both processes. The thrust angle (θ_T) is utilized to exploit these correlations; θ_T is determined for each event as the angle between the momentum vector of the signal photon and the thrust vector [8] calculated using all *other* final state photons and charged particles boosted into the rest frame of the η_b candidate (defined by the signal photon). As shown in Fig. 1(a), the thrust angle distribution for the data events is peaked near $|\cos\theta_T| = 1$, whereas the thrust angle for the η_b signal events from Monte Carlo (MC) simulations is distributed uniformly. As a result, the sensitivity to a possible η_b signal in the presence of background varies greatly with $|\cos\theta_T|$, and it can be maximized by taking advantage of the $|\cos\theta_T|$ distribution.

We utilize the $|\cos\theta_T|$ distribution, but in a manner quite different from that used by *BABAR* [5]. Instead of simply rejecting all events with large values of $|\cos\theta_T|$, we increase the sensitivity to η_b by forming three separate photon energy spectra, one each for the $|\cos\theta_T|$ regions (0.0, 0.3) (I), (0.3, 0.7) (II), and (0.7, 1.0) (III), and performing a simultaneous joint fit to all three distributions. The signal-to-background ratio improves from region III to

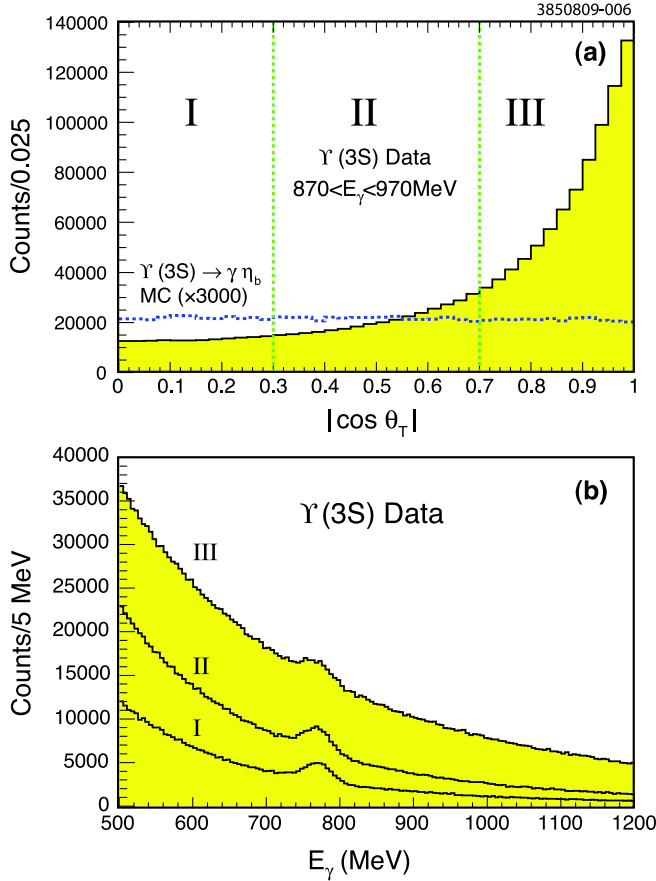


FIG. 1 (color online). (a) Distribution of $|\cos\theta_T|$ for η_b signal MC events (dotted) and background dominated $Y(3S)$ data (shaded) in three regions, I, II, and III defined in the text. The histogram of the Monte Carlo simulation of the $Y(3S) \rightarrow \gamma\eta_b$ signal has been multiplied by a factor of 3000 to make it visible. (b) The E_γ distribution from $Y(3S)$ data in the three regions of $|\cos\theta_T|$. Only the $\chi_{bJ}(2P) \rightarrow \gamma Y(1S)$ lines at around 770 MeV are visible above the background.

region II and from region II to region I, but all regions contribute to the sensitivity. Monte Carlo simulations show that, for a data sample of our size and a $\mathcal{B}(Y(3S) \rightarrow \gamma\eta_b)$ whose value is assumed to be what is measured below, the three-region joint fit procedure leads to an average increase in the statistical significance of an η_b signal of 0.6σ over only accepting events with $|\cos\theta_T| < 0.7$, albeit with a large rms spread of 0.7σ among MC trials. We compute the statistical significance of the fit using the conventional likelihood expression $\sqrt{2 \ln(\mathcal{L}_{\text{sig}}/\mathcal{L}_0)}$, where \mathcal{L}_{sig} is the likelihood of the fit with a signal and \mathcal{L}_0 is the likelihood of the fit with the signal constrained to zero. An average gain in significance over using no information about the thrust axis is 1.7σ with an rms spread of 1.6σ . Most of the 0.6σ increase in sensitivity from the joint fit comes from splitting the $|\cos\theta_T| < 0.7$ region into two bins, which exploits the smaller background relative to expected signal in the $|\cos\theta_T| < 0.3$ bin compared to the $0.3 < |\cos\theta_T| < 0.7$

bin. On the average, inclusion of the $|\cos\theta_T| > 0.7$ region by itself improves the result by 0.2σ .

The photon peaks have shapes which are parametrized by convolving a relativistic Breit-Wigner resonance function with a Crystal Ball (CB) calorimeter response function [9], which consists of a Gaussian part with width σ (the energy resolution) smoothly joined to a low-side power-law tail described by two additional shape parameters. The energy resolution and CB shape parameters were determined with two complementary methods. In Method A, we utilized isolated photons in $e^+e^- \rightarrow e^+e^-\gamma$ data events with photon energies near $E_{\text{true}} = 750$ MeV, where E_{true} is the photon energy expected from using only the measured angles of the e^\pm and γ . We then extracted an inherent line shape by deconvolving the spread in E_{true} (obtained from simulated events) from the observed E_γ/E_{true} . In Method B, we compared exclusive $Y(3S) \rightarrow \gamma\chi_{b1}(2P)$, $\chi_{b1}(2P) \rightarrow \gamma Y(1S)$, $Y(1S) \rightarrow \ell^+\ell^-$ ($\ell^\pm \equiv e^\pm$ or μ^\pm) in data and MC simulation to determine the shape of the $Y(3S) \rightarrow \gamma\chi_{b1}(2P)$ photon line. The data distribution was used to determine the Gaussian part of the shape and the MC simulations were used to determine the two tail parameters after tuning the MC parameters to match the Gaussian part observed in the data. Methods A and B lead to consistent energy resolutions and CB shape parameters, resulting in a line shape that is significantly different from that used in the original CLEO analysis. While the tail parameters of the peak shapes are fixed to be the same for all three relevant photon energies ($\chi_{bJ}(2P)$, ISR, and η_b), the Gaussian widths for the three are different. The fitted Gaussian width for the overlapping $\chi_{bJ}(2P)$ peaks near 770 MeV in the inclusive spectrum is $\sigma(770 \text{ MeV}) = 16.7 \pm 1.0$ MeV. The variation of the photon resolution width with energy was determined from MC simulations made for a wide range of photon energies. Its parametrization was used to obtain the extrapolated values, $\sigma(859 \text{ MeV}) = 17.4 \pm 1.0$ MeV, and $\sigma(920 \text{ MeV}) = 18.3 \pm 1.1$ MeV, for the ISR and η_b peaks, respectively.

The expected intensity of the ISR peak was obtained by extrapolating its yield observed in CLEO data taken on the $Y(4S)$ resonance. The expected yield $N(\text{ISR}) = 1726 \pm 131$, photon energy $E_\gamma(\text{ISR}) = 859$ MeV, and energy resolution $\sigma(\text{ISR}) = 17.4$ MeV are fixed in all fits of the inclusive spectra.

The prominent peaks in the inclusive spectra shown in Fig. 1(b) are composites of the three $\chi_{bJ}(2P) \rightarrow \gamma Y(1S)$ peaks for $J = 0, 1, 2$. We fix the relative strengths of these three lines to the ratios determined from other measurements [10] and float only the overall amplitude. We also fix the spin-orbit splitting of these lines to the values measured in Ref. [4], but we float the absolute energy scale. The latter provides a useful check on our uncertainty in the absolute energy calibration. The CB line shape parameters are fixed as discussed previously, while the effective energy resolution, which includes Doppler smearing, is allowed to float.

The efficiencies for $\chi_{bj}(2P)$, ISR, and η_b in our event selections are obtained by Monte Carlo simulations with the $1 + \alpha \cos^2 \theta$ angular distributions expected for E1 and M1 transitions with appropriate values of α for $\chi_{b1}(2P)$ and $\chi_{b2}(2P)$, and $\alpha = 1$ for $\chi_{b0}(2P)$ and η_b . Separate calculations were done for the three $|\cos \theta_T|$ bins, and it was found that efficiencies are approximately constant in $|\cos \theta_T|$. The summed efficiencies for η_b and ISR are $(54.2 \pm 3.8)\%$ and $(6.9 \pm 0.1)\%$, respectively.

As discussed previously, we perform a joint fit of the data in three $|\cos \theta_T|$ bins. All fitting parameters (apart from those in the background function described below) are constrained to be the same in the three $|\cos \theta_T|$ bins. That is, the yields for the $\chi_{bj}(2P)$, ISR, and η_b photon peaks in each of the three $|\cos \theta_T|$ bins were constrained to be proportional to the ratios $\Delta |\cos \theta_T|_i / \epsilon_i$ where ϵ_i is the signal efficiency for bin i .

The smooth background was fitted with exponential polynomials,

$$\frac{dN}{dE_\gamma} = \exp\left(\sum_{i=0}^n a_i E_\gamma^i\right). \quad (1)$$

As the only experimental handle on these backgrounds is the inclusive spectrum itself, we explored uncertainties in their determination by varying binning types (both linear and logarithmic binning were used), the order of the polynomial (n was varied from 2 to 4 in each thrust bin independently) and the fit range (six different ranges were tried extending down to 500 MeV and up to 1340 MeV). Results for the η_b (mass, significance, and branching fraction) were then averaged through all fits with confidence level (CL) above 10%. The rms spread among the fit variations was taken as a measure of the systematic uncertainty in the background determination. Averaged through all successful fits, the maximum likelihood significance of the η_b signal is 4.1σ with an rms spread of 0.4σ . A representative fit, whose parameters are close to the average values for the ensemble of accepted fits, is chosen as nominal. This fit (shown in Fig. 2) has $N(\gamma\eta_b) = 2311 \pm 546$ counts and gives $\mathcal{B}(\gamma\eta_b) \equiv \mathcal{B}(Y(3S) \rightarrow \gamma\eta_b) = (7.1 \pm 1.8) \times 10^{-4}$ and $E_\gamma(\gamma\eta_b) \equiv E_\gamma(Y(3S) \rightarrow \gamma\eta_b) = 918.6 \pm 6.0$ MeV, with a CL of 18.5%.

The systematic uncertainties in our results are obtained as follows and are summarized in Table I. We assign the rms variations in the results obtained for all the accepted fits, ± 1.0 MeV in $E_\gamma(\gamma\eta_b)$, and $\pm 10\%$ in $\mathcal{B}(\gamma\eta_b)$ as systematic uncertainties due to background shape, binning, and range variations. The changes in our results are negligible when we alter the lower CL limit for acceptable fits from 10% to either 5% or 15%. We vary the photon energy resolution, the Crystal Ball shape parameters, and the $\chi_{bj}(2P)$ parameters within their errors and assign the resulting variations in $E_\gamma(\gamma\eta_b)$ and $\mathcal{B}(\gamma\eta_b)$ as systematic uncertainties.

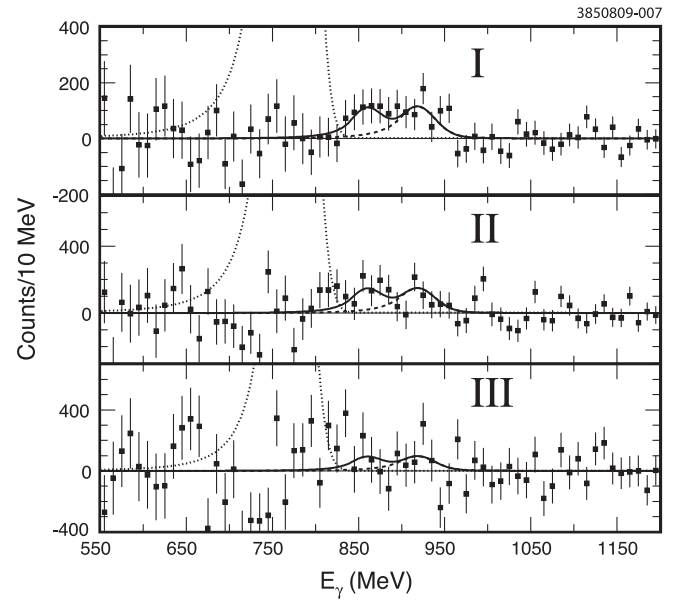


FIG. 2. Background- and $\chi_{bj}(2P)$ -subtracted distributions of E_γ from $Y(3S)$ decays in three $|\cos \theta_T|$ regions, I, II, and III defined in the text. The curves are the results of the joint fit, with a CL of 18.5%. The $\chi_{bj}(2P)$ peaks are indicated by the dotted lines and the η_b signals by the dashed lines, which join the solid line.

The fitted $\chi_{bj}(2P)$ centroid energy in our data is 769.9 ± 0.2 MeV, while the expected energy is $769.6^{+0.7}_{-1.0}$ MeV. The 0.3 MeV deviation of our measured value suggests that our photon energy calibration has a maximum possible uncertainty of $^{+0.9}_{-1.2}$ MeV. This is consistent with our measurement of ISR photon energies from $Y(4S)$ and below $Y(4S)$ data, which agree with the expected energies within ± 0.3 MeV. Based on these considerations we conservatively assign the systematic uncertainty due to photon energy calibration as ± 1.2 MeV. We obtained the value

TABLE I. Summary of estimated systematic uncertainties and their sums in quadrature for the $Y(3S) \rightarrow \gamma\eta_b$ analysis. The item labeled Background refers to variations of the background function parameters, the fit range, and linear versus logarithmic E_γ binning.

Source	Uncertainty in	
	$E_\gamma(\gamma\eta_b)$ (MeV)	$\mathcal{B}(\gamma\eta_b)$ (%)
Background	± 1.0	± 10
Photon Energy Calibration	± 1.2	-
Photon Energy Resolution	± 0.3	± 2
CB and $\chi_{bj}(2P)$ Parameters	± 0.7	± 8
ISR Yield	± 0.4	± 3
Photon Reconstruction	-	± 2
$N(Y(3S))$	-	± 2
MC Efficiency	-	± 7
η_b Width	± 0.6	± 9
Quadrature sums	± 1.9	± 18

of $\mathcal{B}(\gamma\eta_b)$ by assuming $\Gamma(\eta_b) = 10 \text{ MeV}/c^2$. We find that $\mathcal{B}(\gamma\eta_b)$ depends linearly on the assumed value of $\Gamma(\eta_b)$ in MeV/c^2 , as $\mathcal{B}(\gamma\eta_b) = [5.8 + 0.13\Gamma(\eta_b)] \times 10^{-4}$. Varying $\Gamma(\eta_b)$ from 5 to 15 MeV/c^2 , a range that includes nearly all theoretical expectations [11], the branching fraction changes by $\pm 0.65 \times 10^{-4}$ or $\pm 9\%$. This uncertainty in the η_b width also contributes $\pm 0.6 \text{ MeV}$ to the uncertainty in $E_\gamma(\gamma\eta_b)$. Other systematic uncertainties are due to the Monte Carlo efficiency calculation and the number of $Y(3S)$ events.

In fitting the $\gamma\eta_b$ peaks, we do not include the factor [12] $(E_\gamma/E_0)^3[1 + \alpha(E_\gamma/E_0)^2]$ expected in the decay width for the hindered M1 transition $Y(3S) \rightarrow \gamma\eta_b$. (E_0 is the photon energy for the central value of the η_b mass.) While theoretical estimates [12] of α vary, $\alpha = 1$ leads to a distortion of the η_b peak shape and a consequent reduction of $E_\gamma(\gamma\eta_b)$ by approximately 3 MeV. Since our data sample is not large enough to determine α , in the absence of firm theoretical predictions we do not include this effect as a bias or as a term in our systematic error.

Our final results are: $E_\gamma(\gamma\eta_b) = 918.6 \pm 6.0 \pm 1.9 \text{ MeV}$ and $\mathcal{B}(\gamma\eta_b) = (7.1 \pm 1.8 \pm 1.3) \times 10^{-4}$, where the first errors are statistical and the second errors are systematic. Our result for $E_\gamma(\gamma\eta_b)$ corresponds to $M(\eta_b) = 9391.8 \pm 6.6 \pm 2.0 \text{ MeV}/c^2$ and $\Delta M_{\text{hf}}(1S)_b = 68.5 \pm 6.6 \pm 2.0 \text{ MeV}/c^2$. This is consistent with lattice QCD predictions that employ dynamical quarks and include both continuum and chiral extrapolations [13]. Our results for both $\Delta M_{\text{hf}}(1S)_b$ and $\mathcal{B}(\gamma\eta_b)$ are also well within the wide range of pQCD based theoretical predictions [14]. Both measurements are in good agreement with the BABAR measurements [5,6].

We also analyzed our data set containing $(9.32 \pm 0.19) \times 10^6$ $Y(2S)$ events for $Y(2S) \rightarrow \gamma\eta_b$ using the same event selection and joint fit analysis procedure as described above for $Y(3S) \rightarrow \gamma\eta_b$. One difference is that we chose to represent the $Y(2S) \rightarrow \pi^0\pi^0Y(1S)$ background component explicitly in the fit since it introduces a kink in the spectrum not far from the signal region. The shape of this background was taken from Monte Carlo simulations. Its normalization was fixed to the PDG value of the branching fraction. Unlike in the $Y(2S)$ analysis, the addition of the explicit $Y(3S) \rightarrow \pi^0\pi^0Y(1S)$ background component to the $Y(3S)$ fits had a negligible effect on the

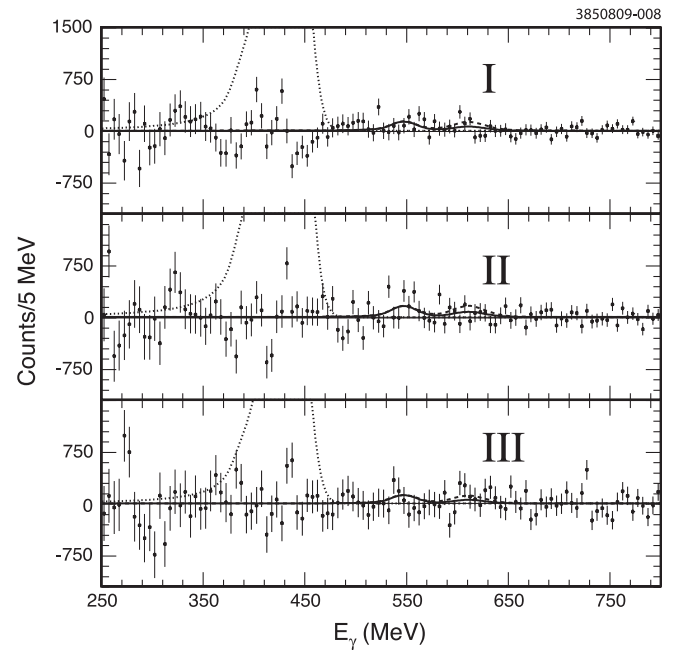


FIG. 3. Background- and $\chi_{bj}(2P)$ -subtracted distributions of E_γ from $Y(2S)$ decays in three $|\cos\theta_T|$ regions, I, II, and III defined in the text. The curves are the joint fit results. The $\chi_{bj}(1P)$ peaks are indicated by the dotted lines and the 90% η_b upper limits by the dashed lines.

results. In the expected signal region for $Y(2S)$ radiative decay, $200 < E_\gamma < 800 \text{ MeV}$, the background is an order of magnitude larger than in the $Y(3S)$ signal region, and in none of the $Y(2S)$ $|\cos\theta_T|$ regions could the η_b be identified. In the joint fit analysis (shown in Fig. 3), fixing $E_\gamma(Y(2S) \rightarrow \gamma\eta_b) = 611 \text{ MeV}$, corresponding to η_b mass determined in $Y(3S)$ decay, leads to $\mathcal{B}(Y(2S) \rightarrow \gamma\eta_b) = (3.9 \pm 2.7 \pm 2.3) \times 10^{-4}$, or an upper limit of $\mathcal{B}(Y(2S) \rightarrow \gamma\eta_b) < 8.4 \times 10^{-4}$ at 90% confidence level. This is consistent with the BABAR $Y(2S)$ result [6], $\mathcal{B}(Y(2S) \rightarrow \gamma\eta_b) = (3.9_{-1.0}^{+1.1} \pm 0.9) \times 10^{-4}$.

We gratefully acknowledge the effort of the CESR staff in providing us with excellent luminosity and running conditions. This work was supported by the A.P. Sloan Foundation, the National Science Foundation, the U.S. Department of Energy, the Natural Sciences and Engineering Research Council of Canada, and the U.K. Science and Technology Facilities Council.

- [1] P. Franzini *et al.* (CUSB Collaboration), Phys. Rev. D **35**, 2883 (1987).
 [2] A. Heister *et al.* (ALEPH Collaboration), Phys. Lett. B **530**, 56 (2002).

- [3] J. Abdallah *et al.* (DELPHI Collaboration), Phys. Lett. B **634**, 340 (2006).
 [4] M. Artuso *et al.* (CLEO Collaboration), Phys. Rev. Lett. **94**, 032001 (2005).

G. BONVICINI *et al.*PHYSICAL REVIEW D **81**, 031104(R) (2010)

- [5] B. Aubert *et al.* (BABAR Collaboration), Phys. Rev. Lett. **101**, 071801 (2008).
- [6] B. Aubert *et al.* (BABAR Collaboration), Phys. Rev. Lett. **103**, 161801 (2009).
- [7] Y. Kubota *et al.* (CLEO Collaboration), Nucl. Instrum. Methods Phys. Res., Sect. A **320**, 66 (1992); M. Artuso *et al.*, Nucl. Instrum. Methods Phys. Res., Sect. A **554**, 147 (2005); D. Peterson *et al.*, Nucl. Instrum. Methods Phys. Res., Sect. A **478**, 142 (2002).
- [8] S. Brandt *et al.*, Phys. Lett. **12**, 57 (1964); E. Farhi, Phys. Rev. Lett. **39**, 1587 (1977).
- [9] J.E. Gaiser *et al.*, Phys. Rev. D **34**, 711 (1986); also J.E. Gaiser, Ph.D. thesis, Stanford University, 1982 [SLAC Report No. SLAC-R-255 (unpublished)].
- [10] C. Amsler *et al.* (Particle Data Group), Phys. Lett. B **667**, 1 (2008), and 2009 partial update for the 2010 edition.
- [11] W. Kwong, P.B. Mackenzie, R. Rosenfeld, and J.L. Rosner, Phys. Rev. D **37**, 3210 (1988); C.S. Kim, T. Lee, and G.L. Wang, Phys. Lett. B **606**, 323 (2005); J.P. Lansberg and T.N. Pham, Phys. Rev. D **75**, 017501 (2007).
- [12] V. Zambetakis and N. Byers, Phys. Rev. D **28**, 2908 (1983); D. Ebert, R.N. Faustov, and V.O. Galkin, Phys. Rev. D **67**, 014027 (2003).
- [13] A. Gray *et al.* (HPQCD and UKQCD Collaborations), Phys. Rev. D **72**, 094507 (2005); T. Burch *et al.*, arXiv:0911.0361v1.
- [14] S. Godfrey and J.L. Rosner, Phys. Rev. D **64**, 074011 (2001); **65**, 039901(E) (2002).